A structural study of the tensile drawing behaviour of poly(ethylene terephthalate)

S. R. Padibjo and I. M. Ward
Department of Physics, University of Leeds, Leeds LS2 9JT, UK
(*Received* 3 *September* 1982)

A study of single-stage and two-stage drawing of poly(ethylene terephthalate) has been undertaken. Measurements of the modulus of the drawn films were combined with a range of structural measurements, including refractive index, X-ray diffraction and infra-red spectroscopy. The development of molecular orientation during drawing is discussed in terms of the deformation of a molecular network, and reasons for the differences between single stage and two-stage drawing are proposed. The relationships between different measures of molecular orientation are considered with the aim of obtaining an understanding of the factors which influence the modulus values. It appears that the modulus relates primarily to the molecular chains which are in the extended *trans* conformation, irrespective of crystallinity.

Keywords Poly(ethylene terephthalate); tensile drawing; structural study; X-ray diffraction; infra-red spectroscopy

INTRODUCTION

The drawing behaviour of poly(ethylene terephthalate) (PET) has been studied extensively over many years, and different workers have highlighted different features, from the purely mechanical aspects[1] to the structural changes which occur[2], and the relationship between properties, especially modulus, and the development of an oriented structure[3,4]. The use of infra-red spectroscopy has proved of particular interest, especially since the recognition of the importance of changes in molecular conformation[5], and this approach has been followed by several workers[6,7].

In this paper, an account will be given of recent studies of single stage and two-stage drawing of PET, with particular reference to two aspects. In the first instance there is the development of molecular orientation and concomitant changes in molecular conformation, which have been examined by X-ray diffraction, infra-red spectroscopy and optical measurements. Particular attention has been given to the interpretation of drawing in terms of a molecular network, first suggested on the basis of the early infra-red studies[2], and confirmed by more recent investigations[7,8]. Secondly, there is the structural interpretation of the increase in modulus with increasing draw ratio and orientation, which will be considered in the light of the results obtained.

EXPERIMENTAL

Preparation of oriented films

For the single stage drawn films, a wide ($\sim$6 cm) sheet of amorphous PET was produced by melt extrusion at 290°C through a slit die followed by quenching onto a chill roll at 20°C. The sheet had a thickness of $\sim 70\,\mu$m and a birefringence less than 0.001. The PET polymer was Diolen 174 (ENKA BV., Arnhem, Holland) with a relative viscosity in *m*-Cresol of 1.85 dl/g.

Dumbbell samples with gauge length dimensions 1 cm width and 10 cm length were then drawn on an Instron tensile testing machine at 80°C and 85°C, at a constant crosshead speed of 4 cm/min, to a series of draw ratios.

For the two stage drawn films, a tape of amorphous PET was produced by melt extrusion of the same polymer at 280°C through a slit die followed by quenching into a water bath. The tape cross-section was 55 μm $\times$ 1.25 mm, and the birefringence was again less than 0.001.

To produce two-stage drawn films, the tape was first stretched between moving rollers in a continuous draw-frame to a draw ratio of 2.25 through a water bath, maintained at constant temperatures of 80°C and 85°C. The resulting drawn tape was then drawn again in an Instron tensile testing machine at the same temperature as in the first drawing stage. The sample gauge length was again fixed at 10 cm, and the cross head speed fixed at 4 cm/min.

Wide films were used for the single stage drawing process where this was possible. Narrow tapes were required for the first stage continuous drawing process for the two-stage drawn films, although they were not ideal for the infra-red measurements, where it was necessary to make a grid of parallel tapes to utilize the full spectrometer beam. The structural studies to be discussed show that both types of film possess fibre symmetry.

Measurement of birefringence

The refractive indices n_z parallel to the draw direction and n_x perpendicular to the draw direction in the plane of the film were measured by an image splitting Zeiss Jena Interphako interference microscope, with 'Cargille' standard refractive index liquids. All measurements were made at 551 nm.

Measurement of density

The sample densities were measured with a density gradient column prepared from a mixture of carbon tetrachloride and n-heptane.

0032-3861/83/091103-10$03.00

Measurement of modulus

For measurement of modulus, the sample of drawn film was tightly clamped between layers of emery paper in specially made light clamps, so that a taut gauge length of 5.0 cm was produced. The sample was extended in an Instron tensile testing machine at a crosshead speed of 0.5 cm/min, with a fast chart recorder speed of 60 cm/min to give a highly resolved load-extension curve. The modulus was then determined from the initial tangent line on the linear portion of the load-extension curve.

Infra-red measurements

The infra-red spectra of the drawn films were measured using a Grubb-Parsons double beam grating spectrometer (Spectromajor) equipped with a wire grid polarizer (Cambridge Consultants Ltd., Type 1CR55). For each sample two spectra were recorded over the range 750–1100 cm^{-1}, with the electric vector parallel to the draw direction (z) or perpendicular to the draw direction in the plane of the film (x). The scan speed was standardized at 50 cm^{-1}/min with a normal slit programme reducing the entrance slit width from ~1 mm at 750 cm^{-1} to ~0.5 mm at 1100 cm^{-1}.

In this paper we have followed the procedures of previous publications[7,9] and undertaken quantitative measurements on three absorption bands only. These are the bands at 975 cm^{-1} and 898 cm^{-1} which have been assigned to vibrations associated with the *trans* and *gauche* conformations respectively of the

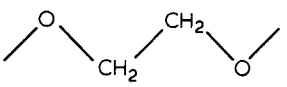

group in the PET chain, and a band at 795 cm^{-1} which has been assigned to a benzene ring vibration and which will be used as an internal standard for determination of film thickness.

For the two stage drawn films, the infra-red samples were prepared by carefully mounting parallel strips side by side on a sample holder. To ensure that there were no gaps, some overlapping between the edges of the strips was inevitable. The sample thickness was therefore determined using the 795 cm^{-1} band as an internal standard, calibrating with single stage drawn films of different thicknesses.

The chart recorder was calibrated on a linear vertical scale so that the ratio I_T/I'_T could be determined directly from the infra-red absorption curve, using a pseudo-base line as described in the previous publication. I'_T is the transmitted intensity at peak absorbance, and I_T the intensity on the pseudo-base line at this frequency. Absorption coefficients k_z and k_x were calculated from equation (12) of a previous publication[9]. For small values of k, the absorbance A is given by

$$A=\log_{10}\left(\frac{I_T}{I'_T}\right)=0.4343\left(\frac{4\pi k y_0}{\lambda}\right)$$

where y_0 is the thickness of the sample and λ is the free space wavelength.

These values of k_z and k_x are then combined with the optical values of n_z and n_x, to obtain the imaginary parts $\langle\alpha''_z\rangle$ and $\langle\alpha''_x\rangle$ of the corresponding average complex polarizabilities, using the Lorentz–Lorenz equation.

For small values of the absorption coefficients we have

$$\frac{6k_z n_z}{(n_z^2+2)}=\frac{4\pi N}{3}\langle\alpha''_z\rangle=\phi_z$$

and

$$\frac{6k_x n_x}{(n_x^2+2)}=\frac{4\pi N}{3}\langle\alpha''_x\rangle=\phi_x$$

where N is the concentration of absorbing species/unit volume and ϕ_z and ϕ_x are the volume polarizabilities.

Following the procedures outlined in a previous paper[9], the refractive index measurements were used to confirm that these films possess transverse isotropy. Then ϕ_z and ϕ_x can be used to find two quantities of immediate physical interest. First, the concentration of absorbing species/unit volume is proportional to $\phi_0=\frac{1}{3}(\phi_z+2\phi_x)$.

Secondly, the orientation of the absorbing species can be defined by an orientation function $\langle P_2(\theta)\rangle_{\text{i.r.}}$ where θ is the angle between the symmetry axis of an absorbing unit (assumed to be transversely isotropic) and the draw direction. The quantity $\langle P_2(\theta)\rangle_{\text{i.r.}}=\frac{1}{2}(3\langle\cos^2\theta\rangle_{\text{i.r.}}-1)$ then defines the mean value of $P_2(\theta)$ determined by infra-red spectroscopy for the aggregate of absorbing species in the drawn sample.

It was shown in the previous paper[9] that

$$\frac{\phi_z-\phi_x}{\phi_z+2\phi_x}=P_2(\theta_m)\langle P_2(\theta)\rangle_{\text{i.r.}}$$

where $P_2(\theta_m)=\frac{1}{2}(3\cos^2\theta_m-1)$ is determined by the angle θ_m which the direction of the dipole moment change makes with the symmetry axis of the absorbing species.

X-ray measurements

Wide-angle X-ray diffraction measurements of crystalline orientation were carried out using a Phillips diffractometer equipped with a quartz monochromator. To determine quantitative values for the crystalline orientation function f_c, azimuthal scans of the $\bar{1}05$ reflection were performed. The data was obtained and processed in the laboratories of ENKA BV, Arnhem, Holland, using fitting procedures described by Heuval and Huisman elsewhere[10,11]. We are indebted to Drs Heuval and Huisman for their assistance in carrying out these measurements. For the lowest draw ratio samples, the crystallinity was too low to permit accurate determination of the crystalline orientation function. The values for f_c included in *Tables 1* and *2* were therefore deduced from data on fibre samples prepared in an identical fashion to the films.

RESULTS AND DISCUSSION

General features of drawn films

Figures 1a and *b* show plots of birefringence as a function of draw ratio for single-stage and two-stage drawing at 80°C and 85°C respectively. In all cases there is a steep initial rise in birefringence at low draw ratios followed by a region of much lower slope at high draw ratios. At a given draw ratio, the two-stage drawn samples always show a lower birefringence than the corresponding single stage samples. This can be attributed to the loss of

Table 1 Calculated data for PET film drawn at 80°C

Sample*	$\langle P_2(\theta)\rangle_{opt}$	x_{cryst}	$\langle P_2(\theta)\rangle_{cryst}$	x_{trans}	x_{gauche}	$\langle P_2(\theta)\rangle_{trans}$	x^{trans}_{amorph}	$\langle P_2(\theta)\rangle^{trans}_{amorph}$
Single-stage drawing:								
3.0/80	0.320	0.04	0.92	0.36	0.64	0.63	0.32	0.59
3.5/80	0.440	0.10	0.92	0.44	0.56	0.78	0.35	0.72
4.0/80	0.554	0.15	0.92	0.54	0.46	0.87	0.39	0.85
4.5/80	0.667	0.19	0.93	0.60	0.40	0.94	0.41	0.94
5.5/80	0.756	0.30	0.93	0.72	0.28	0.97	0.42	1.00†
6.0/80	0.790	0.34	0.93	0.76	0.24	0.99	0.42	1.0(3)†
Two-stage drawing:								
3.0/80	0.220	0.01	0.82	0.30	0.70	0.61	0.29	0.60
3.5/80	0.310	0.02	0.89	0.34	0.66	0.81	0.32	0.81
4.0/80	0.425	0.05	0.90	0.43	0.57	0.91	0.38	0.91
4.5/80	0.510	0.10	0.90	0.49	0.51	0.96	0.39	0.98
5.5/80	0.640	0.19	0.91	0.62	0.38	0.99	0.43	1.0(2)†
6.0/80	0.660	0.21	0.91	0.66	0.34	1.00	0.45	1.0(4)†
6.5/80	0.700	0.23	0.91	0.70	0.30	1.00	0.47	1.0(4)†
7.0/80	0.730	0.24	0.92	0.72	0.28	1.00	0.48	1.0(4)†

* As usual designation 3.0/80 indicates that the sample has been drawn to a total draw ratio of 3.0 at draw temperature of 80°C
† Calculated values, actual value cannot exceed unity

Table 2 Calculated data for PET film drawn at 85°C

Sample	$\langle P_2(\theta)\rangle_{opt}$	x_{cryst}	$\langle P_2(\theta)\rangle_{cryst}$	x_{trans}	x_{gauche}	$\langle P_2(\theta)\rangle_{trans}$	x^{trans}_{amorph}	$\langle P_2(\theta)\rangle^{trans}_{amorph}$
Single-stage drawing:								
3.0/85	0.259	0.02	0.90	0.33	0.67	0.48	0.31	0.45
3.5/85	0.371	0.06	0.91	0.39	0.61	0.66	0.33	0.61
4.0/85	0.449	0.14	0.92	0.49	0.51	0.74	0.35	0.67
4.5/85	0.648	0.19	0.92	0.59	0.41	0.86	0.40	0.83
5.5/85	0.774	0.23	0.93	0.71	0.29	0.88	0.48	0.86
6.0/85	0.815	0.27	0.93	0.75	0.25	0.90	0.48	0.88
Two-stage drawing:								
3.0/85	0.112	0.00	0.83	0.25	0.75	0.69	0.25	0.69
3.5/85	0.163	0.01	0.83	0.26	0.74	0.72	0.25	0.72
4.0/85	0.222	0.02	0.85	0.29	0.71	0.80	0.27	0.80
4.5/85	0.325	0.03	0.85	0.35	0.65	0.90	0.33	0.88
5.5/85	0.496	0.08	0.87	0.50	0.50	0.99	0.42	1.0(1)†
6.0/85	0.562	0.12	0.91	0.55	0.45	1.00	0.43	1.0(2)†
6.5/85	0.600	0.14	0.92	0.57	0.43	1.00	0.43	1.0(2)†
7.0/85	0.720	0.18	0.93	0.64	0.36	1.00	0.46	1.0(3)†

† Calculated values, actual value cannot exceed unity

orientation which occurs when the two-stage drawn samples are being brought to temperature equilibrium in the Instron after the first drawing stage, prior to the second drawing stage. The curves for the two processes can in fact be brought into coincidence in an empirical fashion if it is assumed that the effective draw ratio in the two-stage process $\lambda_{effective} = 0.7\ \lambda_{actual}$, where λ_{actual} is the total draw ratio in this process. This is shown in *Figures 1a* and *1b*.

In *Figure 2* the densities are plotted as a function of draw ratio for drawing at 85°C. The curves are sigmoidal, with a very rapid rise in a comparatively narrow range of draw ratios. This rise marks the onset of crystallinity and occurs at a much higher (total) draw ratio in the two stage drawing process. Similar results are obtained for drawing at 80°C. Again the curves for the two processes may be brought together by the empirical assumption of $\lambda_{effective} = 0.7\ \lambda_{actual}$.

Figure 3 shows the modulus as a function of draw ratio for films drawn at 80°C. It can be seen that these curves are also sigmoidal in shape, and that the rise in modulus also occurs at a higher total draw ratio in the two-stage drawing process. Moreover, it appears from *Figure 3a* that the final saturation level of modulus may be greater for two-stage drawing than for single stage. These curves are different in shape and *Figure 4* shows that they cannot be brought into coincidence by the empirical procedure of an effective draw ratio.

We will therefore consider the structural differences between films drawn by the two routes in order to examine possible explanations of these modulus differences.

Infra-red measurements

In previous infra-red studies on one-way films, it was shown that there was a unique relationship between the proportions of *trans* and *gauche* conformers and the overall orientation[7]. *Figure 5* shows that this result is confirmed for the present films, and is independent of the drawing process. It is also found, as illustrated in *Figure 6a* and *6b* that the development of *trans* orientation is much more rapid than the overall orientation. Although the maximum value for $P_2(\theta_m^{trans})\langle P_2(\theta)\rangle_{trans}$ is similar (~ 0.5 for both single stage and two-stage drawing, it does appear that the two-stage drawing process does produce samples with slightly higher values of infra-red orien-

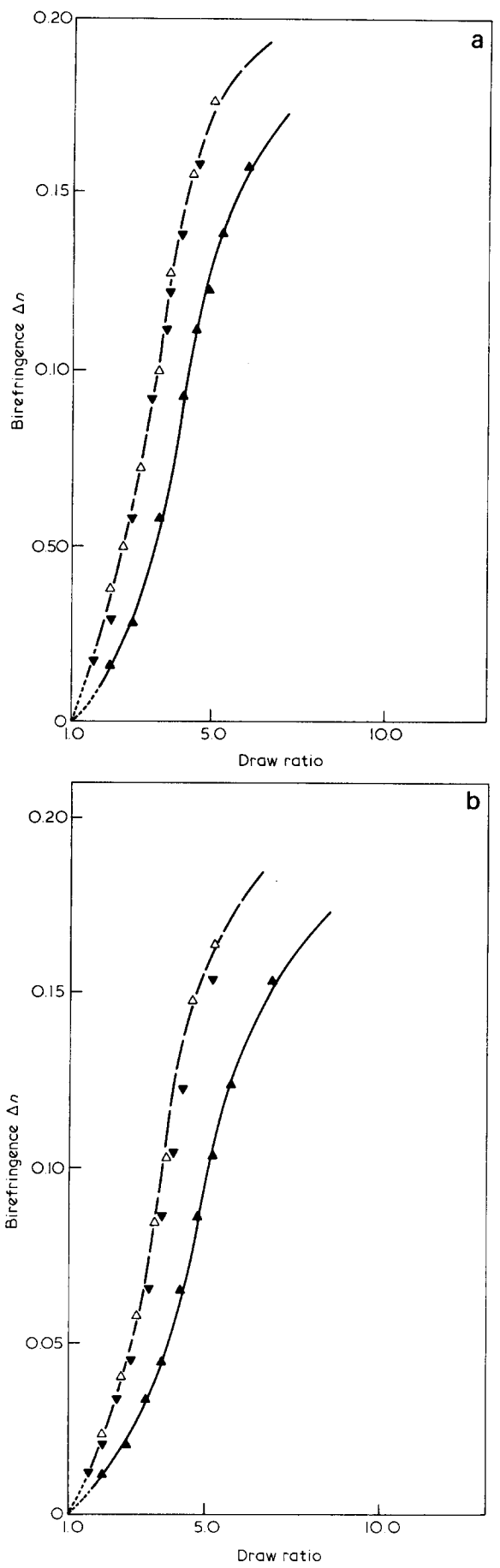

Figure 1 Birefringence *versus* draw ratio for drawn films: △, single-stage; ▲, two stages; ▼, two stages; draw ratio$_{effective}$ = 0.7 draw ratio$_{actual}$ (a) draw temperature 80°C (b) draw temperature 85°C

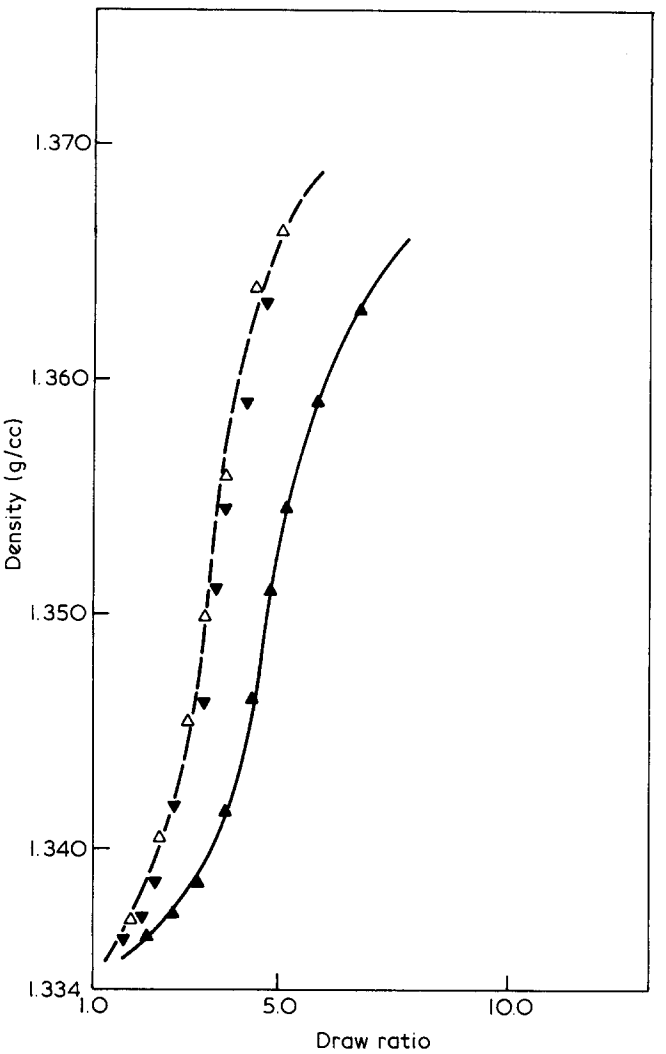

Figure 2 Density *versus* draw ratio for film drawn at 85°C: △, single-stage; ▲, two stages; ▼, two stages; draw ratio$_{eff}$ = 0.7 draw ratio$_{act}$

tation for a given $\langle P_2(\theta)\rangle_{opt}$. This is borne out by a comparison of $x_{trans}\langle P_2(\theta)\rangle_{trans}$ as a function of $\langle P_2(\theta)\rangle_{opt}$. Absolute values of $\langle P_2(\theta)\rangle_{trans}$ were calculated following the procedure of a previous publication[7]. The values of $P_2(\theta_m^{trans})\langle P_2(\theta)\rangle_{trans}$ can be extrapolated to give a constant value for high overall molecular orientation, where it can be assumed that $\langle P_2(\theta)\rangle \rightarrow 1$. The results of the present study are consistent with the previous work in this respect so that a value for θ_m^{trans} of 32° can be assumed. As discussed in a previous paper, if the *gauche* conformers can be assumed to be isotropic $\langle P_2(\theta)\rangle_{opt} = x_{trans}\langle P_2(\theta)\rangle_{trans}$, *Figures 7a* and *7b* show that although this equality holds to a good approximation for all the present samples, the two-stage drawn samples are significantly different from one stage drawn samples.

In several previous publications[7,8,12], it has been shown that the development of orientation in hot drawn samples correspond very well with the deformation of a rubber-like network so that

$$\langle P_2(\theta)\rangle_{opt} = \frac{1}{5N}\left(\lambda^2 - \frac{1}{\lambda}\right)$$

where N is the number of random links between network entanglement points. *Figures 8a* and *8b* show that this

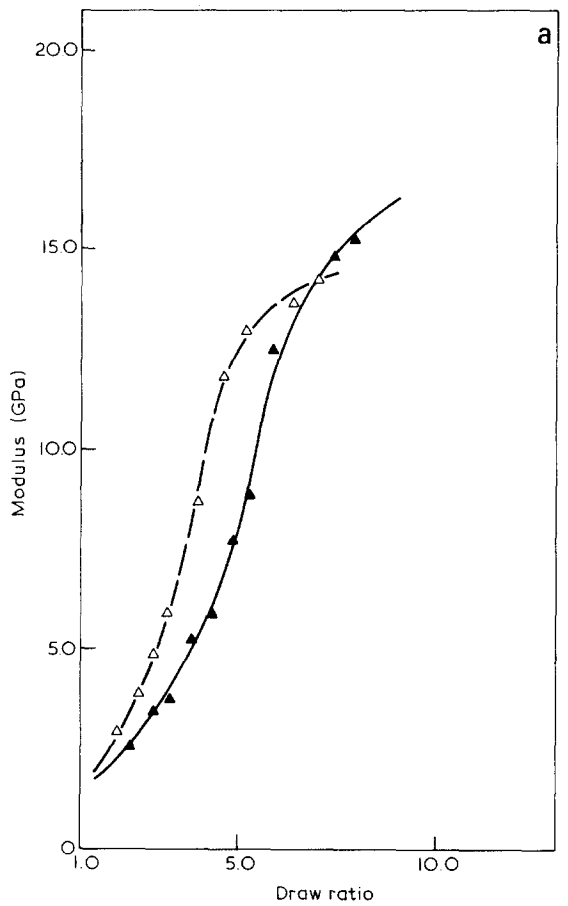

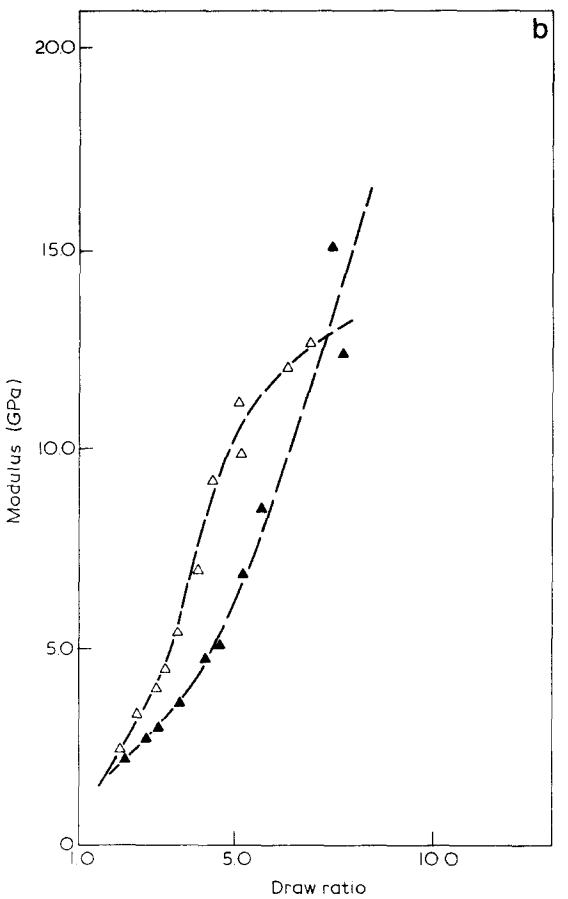

Figure 3 Modulus *versus* draw ratio: △, single stage; ▲, two stages; (a) draw temperature 80°C (b) draw temperature 85°C

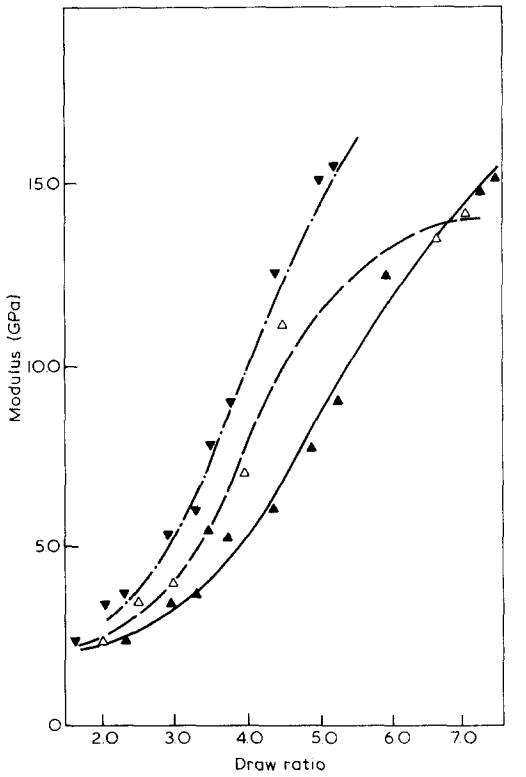

Figure 4 Modulus *versus* draw ratio for draw temperature 80°C: △, single stage; ▲, two stages; ▼, two stages with draw ratio$_{eff}$ = 0.7 draw ratio$_{act}$

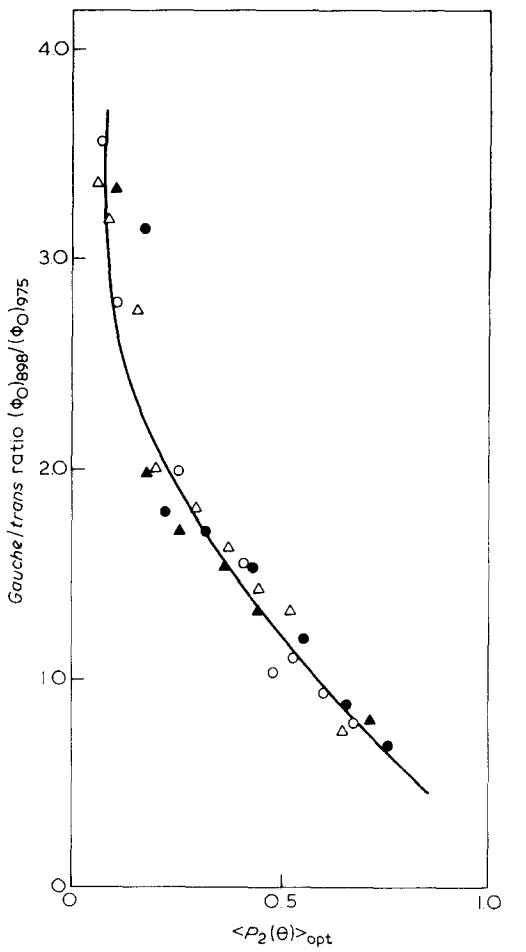

Figure 5 *Gauche/trans* content *versus* $\langle P_2(\theta)\rangle_{opt}$. Circles for draw temperature 80°C, triangles for draw temperature 85°C; full symbols single-stage, open symbols two stages

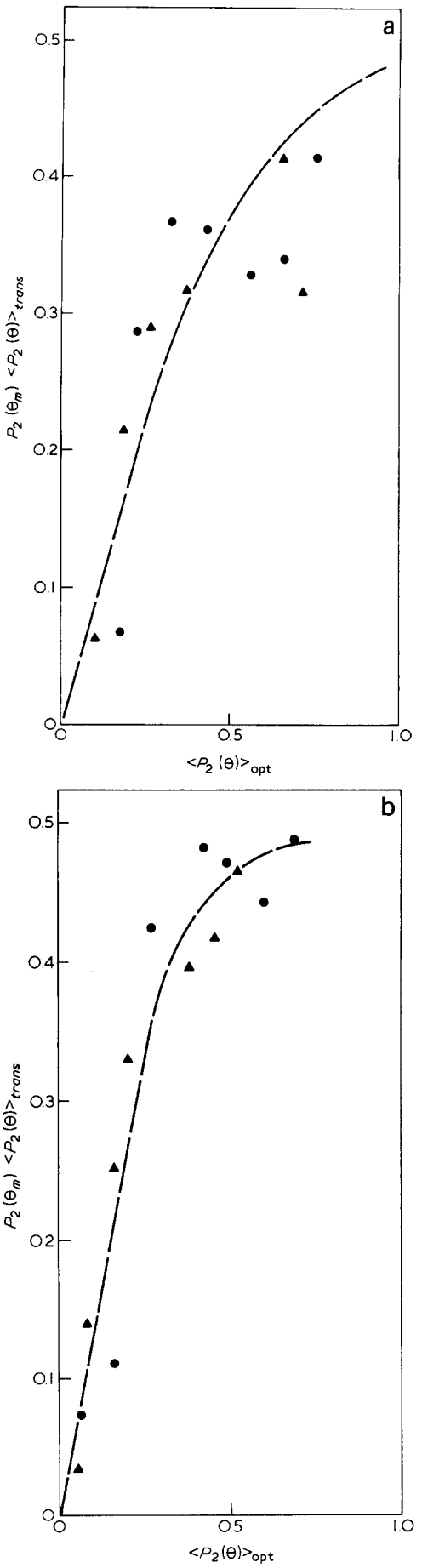

Figure 6 $P_2(\theta)_m\langle P_2(\theta)\rangle_{trans}$ *versus* $\langle P_2(\theta)\rangle_{opt}$. (a) Single-stage draw, (b) two-stages draw: ●, draw temperature 80°C; ▲, draw temperature 85°C

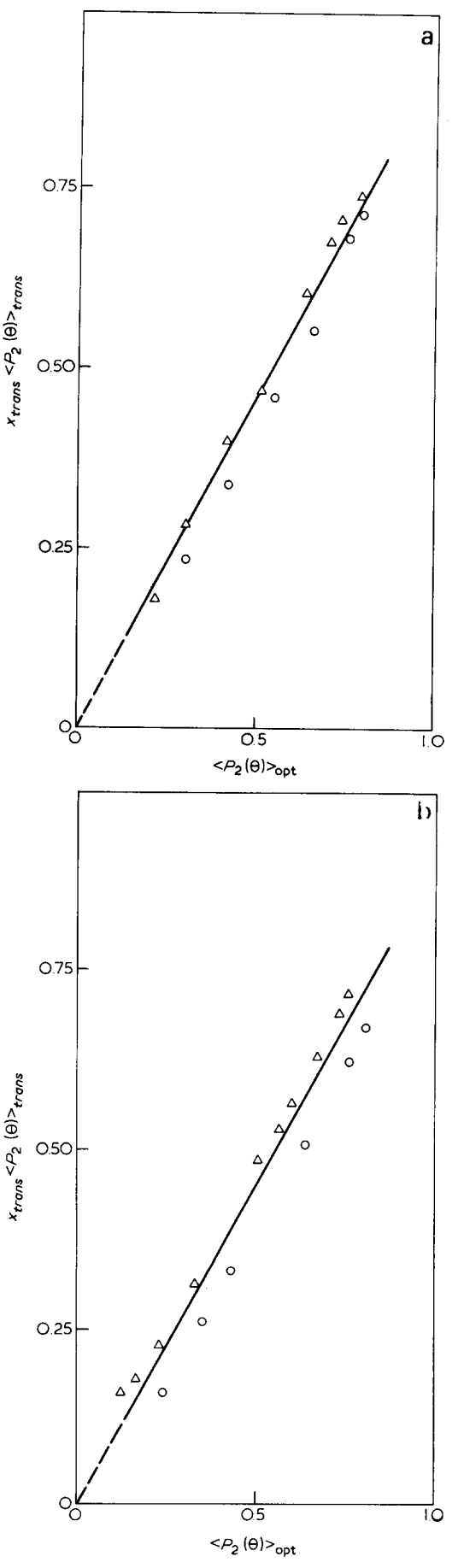

Figure 7 $x_{trans}\langle P_2(\theta)\rangle_{trans}$ *versus* $\langle P_2(\theta)\rangle_{opt}$. (a) Draw temperature 80°C, (b) draw temperature 85°C: ○, single-stage draw; △, two-stage draw

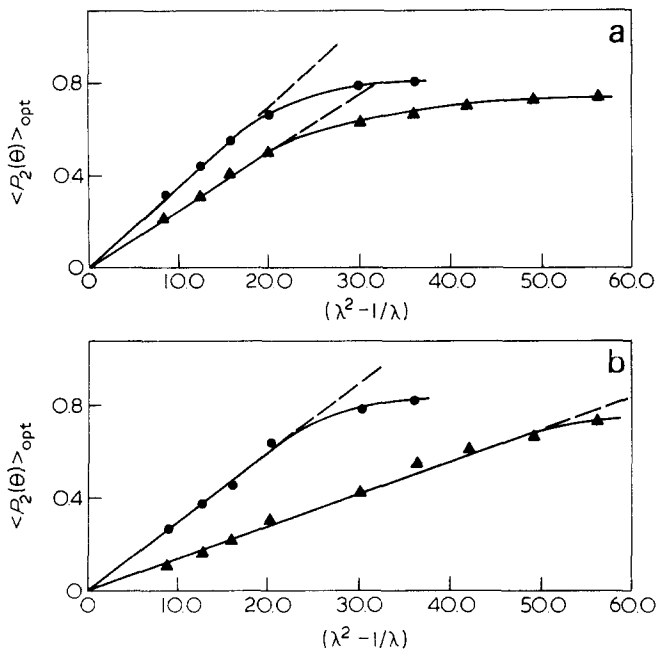

Figure 8 $\langle P_2(\theta)\rangle_{opt}$ *versus* $(\lambda^2 - 1/\lambda)$. (a) Draw temperature 80°C, (b) draw temperature 85°C: ●, single-stage draw; ▲, two-stage draw

relationship holds for these samples up to a limiting draw ratio which increases with increasing draw temperature. At 80°C the limiting draw ratio is *ca.* 4 for single stage drawing and *ca.* 4.5 for two stage drawing. Values of N of about 6 and 8 respectively are obtained from the slopes of these plots for single stage and two-stage drawing respectively. The single stage drawing results correspond very well with previous work[7]. At 85°C the limiting draw ratio is *ca.* 5 for single stage drawing and *ca.* 7 for two-stage drawing with corresponding values for N of about 7 and 14 respectively. To a first approximation the limiting extensibility of the network relates to $N^{\frac{1}{2}}$, so that these results are consistent in a general sense with the two-stage drawing process relating to a looser network. It is also clear from the results shown in *Figure 2* that very appreciable crystallization occurs at draw ratio ~3 for single stage drawing and ~5 for two-stage drawing. This implies that the mechanism of drawing is more complex than the deformation of the original molecular network at draw ratios below which the $\langle P_2(\theta)\rangle_{opt}$ vs. $(\lambda^2 - \lambda^{-1})$ plots cease to be linear.

In this paper the infra-red data can be analysed one stage further than in previous publications. Taking the infra-red and X-ray data together we can consider that there are three components of structure, the crystalline *trans* conformers, the amorphous *trans* conformers and the amorphous *gauche* conformers. The *trans/gauche* ratio can be estimated from the infra-red measurements, and the crystallinity (which gives the crystalline *trans* content) has been determined from the density measurements, using the empirical method of Heuval and Huisman[10,11], which adjusts the amorphous density to allow for increasing amorphous orientation. This correction is similar but smaller numerically than that proposed by Nobbs, Bower and Ward[12]. In view of the comparatively low crystallization of these materials, these small differences do not significantly affect any of our conclusions.

On this scheme, values can be calculated for $\langle P_2(\theta)\rangle^{trans}_{amorphous}$, on the basis that $\langle P_2(\theta)\rangle^{trans}_{cryst}$ is just $\langle P_2(\theta)\rangle_{cryst}$, determined from the X-ray orientation data on the (105) reflection. We have

$$x^{trans} = x^{trans}_{cryst} + x^{trans}_{amor} = x_{cryst} + x^{trans}_{amor} \quad (1)$$

and

$$x^{trans}\langle P_2(\theta)\rangle^{trans} = x_{cryst}\langle P_2(\theta)\rangle_{cryst} + x^{trans}_{amor}\langle P_2(\theta)\rangle^{trans}_{amor} \quad (2)$$

where $\langle P_2(\theta)\rangle^{trans}$ is the orientation average of all the *trans* material including both crystalline and amorphous phases.

The fraction of *trans* material x^{trans} is found from the *trans/gauche* ratio and $x^{trans}_{cryst} = x_{cryst}$ from the density measurements. The quantity x^{trans}_{amor} may then be obtained using equation (1).

$\langle P_2(\theta)\rangle^{trans}$ is determined from the infra-red measurements, and $\langle P_2(\theta)\rangle_{cryst}$ from the X-ray diffraction measurements. Then $\langle P_2(\theta)\rangle^{trans}_{amor}$ is calculated using equation (2). The results of these calculations are summarized in *Tables 1* and *2*. It can be seen that the values of $\langle P_2(\theta)\rangle^{trans}_{amor}$ for the two-stage drawn materials tend to be greater than those for the one-stage drawn materials, especially if compared at comparable values of $\langle P_2(\theta)\rangle_{opt}$ in the range 0.2 to 0.5. The two-stage drawn materials contain a considerable proportion of *trans* conformers which are apparently completely aligned, and a major fraction of these are in the non-crystalline regions.

Orientation of the crystalline and amorphous regions

The crystalline regions are always comparatively highly oriented (*Tables 1* and *2*) with values for $f_c = \langle P_2(\theta)\rangle_{cryst}$ of about 0.90 being obtained even for lower levels of crystallinity.

An amorphous orientation function f_a can be calculated in two ways. First, from the combination of birefringence and X-ray diffraction data, we have

$$\Delta n = x_{cryst} f_c \Delta\hat{n}_c + (1 - x_{cryst}) f_a \Delta\hat{n}_a \quad (3)$$

where $\Delta\hat{n}_c$ and $\Delta\hat{n}_a$ are the maximum birefringences of the crystalline and amorphous phases respectively and x_{cryst} is the fraction of crystalline material.

Thus

$$f_a = \frac{\Delta n - x_{cryst} f_c \Delta\hat{n}_c}{(1 - x_{cryst})\Delta\hat{n}_a} \quad (4)$$

Secondly, we have

$$x_{amor}\langle P_2(\theta)\rangle_{amor} = (1 - x_{cryst})\langle P_2(\theta)\rangle_{amor}$$

$$= x^{trans}_{amor}\langle P_2(\theta)\rangle^{trans}_{amor} + x^{gauche}\langle P_2(\theta)\rangle_{gauche} \quad (5)$$

On the assumption that $\langle P_2(\theta)\rangle_{gauche} = 0$, it then follows that

$$f_a = \langle P_2(\theta)\rangle_{amor} = \frac{x^{trans}_{amor}}{1 - x_{cryst}}\langle P_2(\theta)\rangle^{trans}_{amor} \quad (6)$$

Whereas equation (6) can be calculated directly from all the available data, the evaluation of equation (4) requires the values of $\Delta\hat{n}_c$ and $\Delta\hat{n}_a$. For the purposes of this paper it was assumed that $\Delta\hat{n}_c = 0.235$ and $\Delta\hat{n}_a = 0.275$. These values are consistent with our previous work and recent publications[13-15]. The results of the calculations are

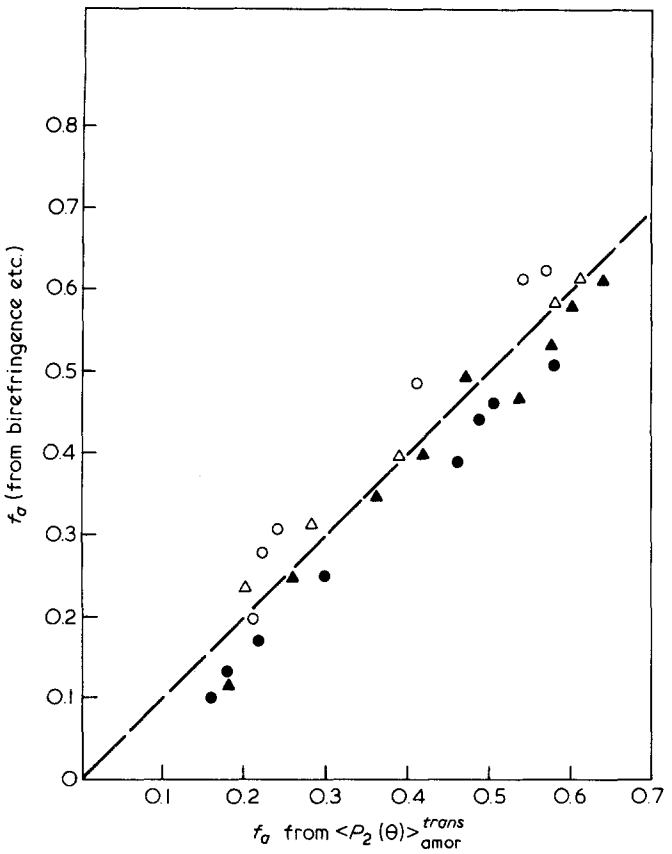

Figure 9 Plot of amorphous orientation average f_a, obtained from birefringence, etc., *versus* f_a obtained from $\langle P_2(\theta)\rangle_{amorph}^{trans}$ etc. Triangles, draw temperature 80°C; circles, draw temperature 85°C: open symbols, single-stage draw; full symbols, two-stage draw

shown in *Figure 9*, where the broken line represents the 1:1 relationship between the two calculated values of f_a. Although there do seem to be small but significant differences between the results for the single and two-stage drawing processes, the overall correlation is very good indeed.

Modulus measurements

Figure 3 shows that the two-stage drawn samples could achieve higher moduli than those for the single stage drawn samples. A most revealing plot is obtained by considering the relationship between final modulus and final crystallinity, which is shown in *Figures 10a* and *10b*. The curves for single stage and two-stage drawing are clearly separated and it appears that the modulus reaches its limiting value for both processes as the crystalline fraction becomes greater than about 0.35. The higher values of modulus achieved by the two-stage drawn materials appear to be related to the lower levels of crystallinity in the latter as the molecular orientation develops. This links with the observation of the higher orientation of *trans* conformers in the amorphous regions in the two-stage drawn materials.

Three possible correlations of the modulus with the structural measurements are presented in *Figures 11*, *12* and *13*. First, there is the correlation between modulus and $x_{trans}\langle P_2(\theta)\rangle_{trans}$, which is seen to be very good indeed, and apparently gives a unique relationship for all samples studied here, irrespective of the drawing process or its temperature. Secondly, *Figures 12* and *13* show that there is not a unique relationship between modulus and the

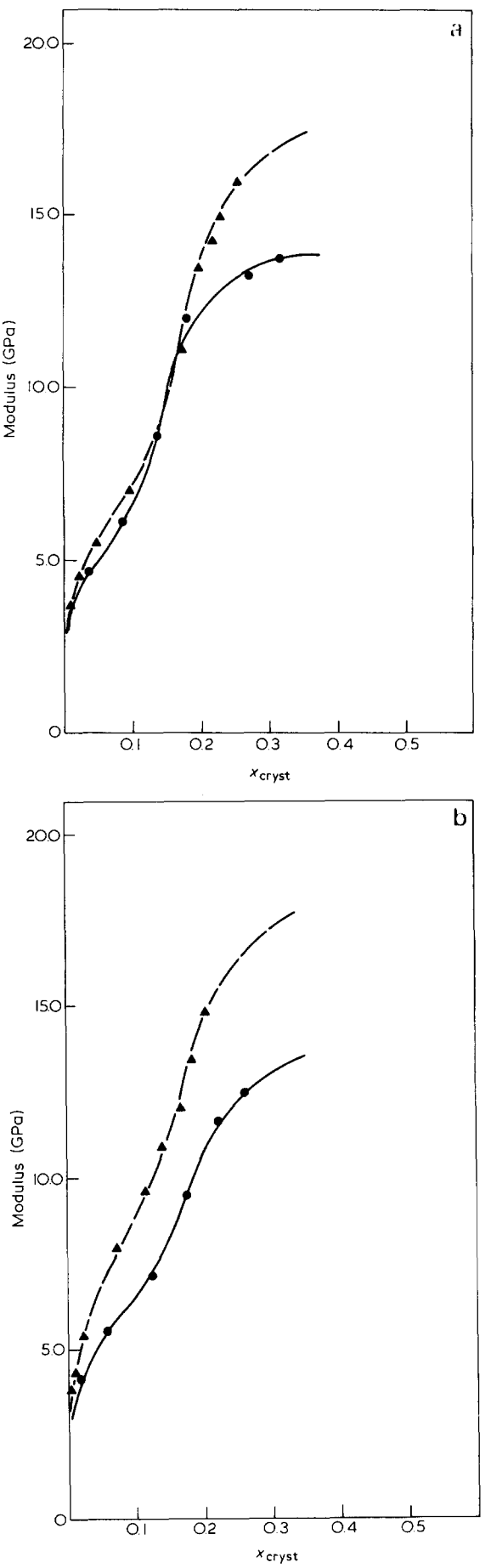

Figure 10 Modulus *versus* crystallinity $x_{cryst.}$ (a) Draw temperature 80°C, (b) draw temperature 85°C: ●, single-stage draw; ▲, two-stage draw

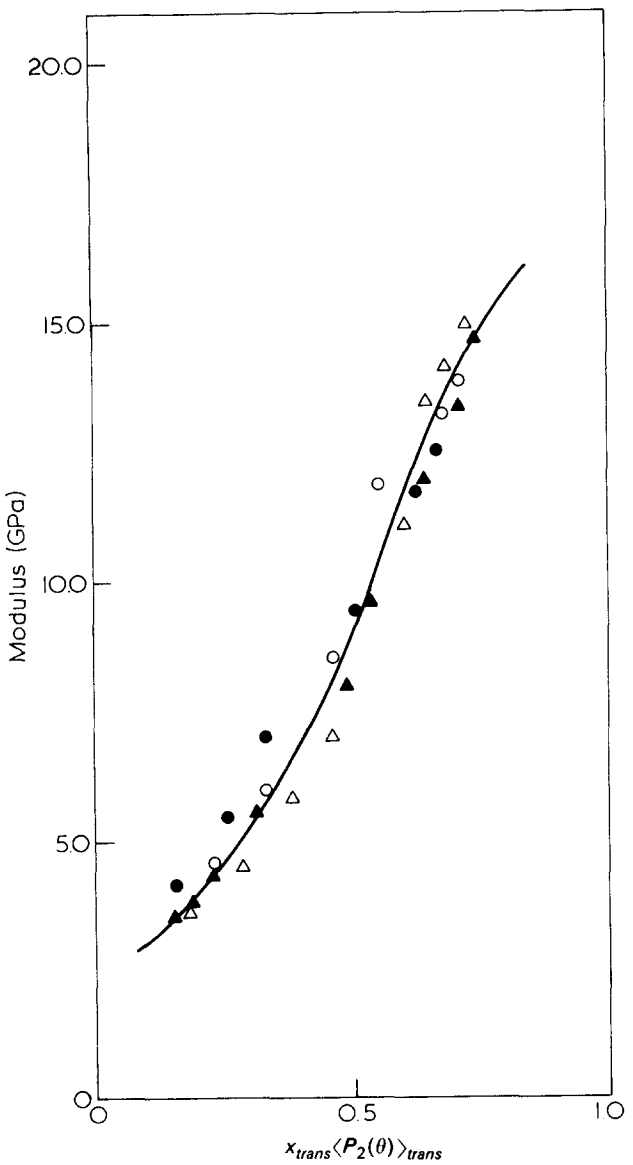

Figure 11 Modulus *versus* $x_{trans}\langle P_2(\theta)\rangle_{trans}$. Circles, single-stage draw; triangles, two-stage draw; open symbols, draw temperature 80°C; full symbols, draw temperature 85°C

amorphous orientation f_a, or between modulus and $x^{trans}_{amor}\langle P_2(\theta)\rangle^{trans}_{amor}$.

It is therefore concluded that the modulus in drawn PET depends primarily on the molecular chains which are in the extended *trans* conformation, irrespective of whether these chains are in a crystalline or amorphous environment. The greater effectiveness of the two stage drawing process appears to arise from the much lower crystallinities developed in the two stage process for a given degree of molecular orientation. This enables a higher degree of *trans* orientation to be achieved and is probably associated with the greater extensibility of the molecular network. These results confirm the known correlation between modulus and birefringence in drawn PET, and elaborate this correlation at a structural level.

CONCLUSIONS

(1) For a wide range of single stage and two-stage drawn films of PET there is a very good correlation between the birefringence and the contribution to the orientation from the *trans* conformers, irrespective of crystallinity. The present studies confirm the previous conclusion, based on

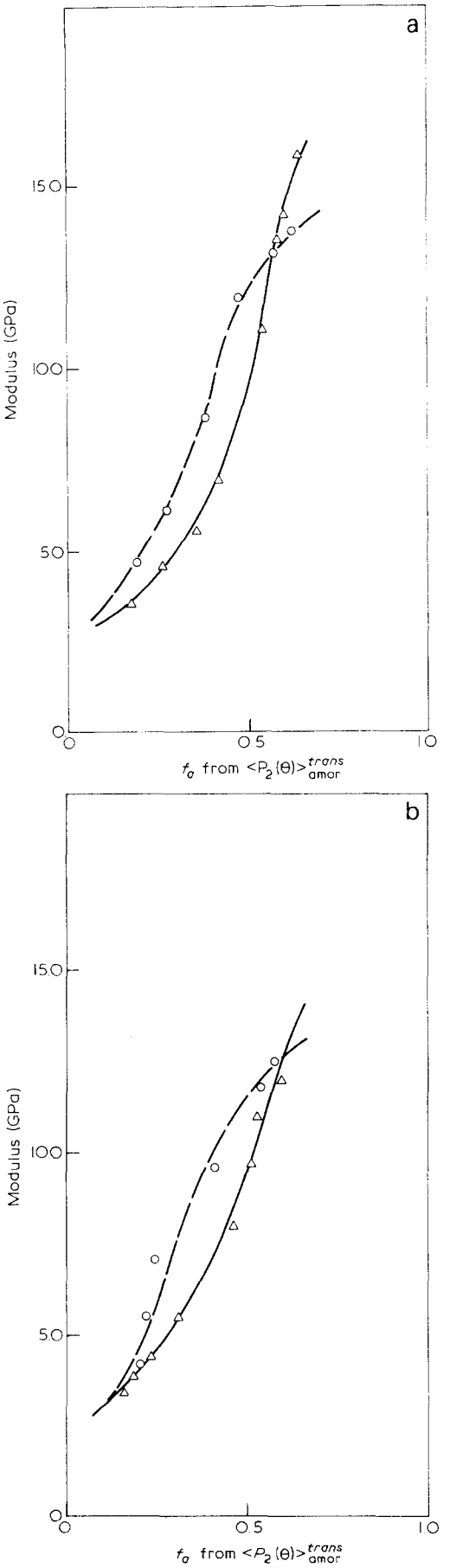

Figure 12 Modulus *versus* f_a from $\langle P_2(\theta)\rangle^{trans}_{amorph}$. Circles, single-stage draw; triangles, two-stage draw: (a) draw temperature 80°C, (b) draw temperature 85°C

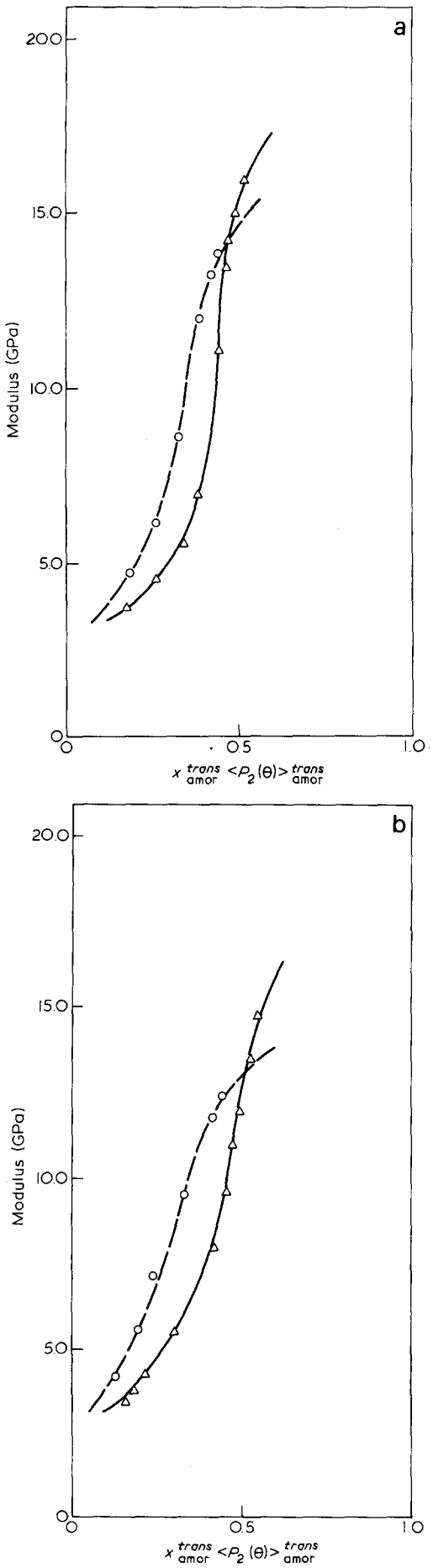

Figure 13 Modulus *versus* $x^{trans}_{amorph}\langle P_2(\theta)\rangle^{trans}_{amorph}$. Circles, single-stage draw; triangles, two-stage draw: (a) draw temperature 80°C, (b) draw temperature 85°C

a much narrower range of samples, that the contribution to the orientation from the *gauche* conformers is very small.

(2) The orientation of the amorphous regions in drawn PET samples has been obtained from infra-red measurements. The results are shown to be in good agreement with values obtained from a combination of birefringence and X-ray diffraction measurements.

(3) The orientation produced in a given drawing process reaches its limiting value when crystallization occurs. Up to the region where this limiting value is approached, drawing corresponds to the stretching of a molecular network. The extensibility of the network can therefore be increased, and hence the modulus of the drawn material, by two-stage drawing where a looser network is obtained and the onset of crystallinity is delayed to higher overall draw ratios. In this connection, it has been shown that the two-stage drawn samples always possess a higher content of amorphous *trans* conformers than the single stage samples, which assists the achievement of a higher overall contribution from molecular chains in the *trans* conformation.

(4) There is an excellent correlation between the modulus of drawn PET and the total contribution to the molecular orientation from the *trans* conformers, irrespective of crystallinity. This correlation is a unique one for all the samples examined. The correlation between modulus and parameters based on amorphous orientation is, on the other hand, poor. A possible explanation is that the drawn PET is essentially a frozen molecular network where the molecular chains associated with oriented amorphous *trans* conformers are as effective as molecular chains in the oriented crystalline regions in contributing to the modulus. The higher modulus of the two-stage drawn samples appears to be associated with the achievement of a higher contribution from amorphous *trans* conformations of the chains before crystallization occurs and locks the molecular network.

ACKNOWLEDGEMENTS

We wish to thank ENKA BV, Arnhem, Holland, for providing financial support for S. R. Padibjo. It is also a pleasure to acknowledge the many useful discussions held with our colleagues at ENKA BV, especially Dr J. Juijn, Dr M. Heuval, Dr H. M. Huisman and Dr M. G. Northolt, whose assistance and collaboration made an invaluable contribution to the research.

REFERENCES

1 Marshall, I. and Thompson, A. B. *Proc. R. Soc. A*, 1954, **221**, 541
2 Farrow, G. and Ward, I. M. *Polymer* 1960, **1**, 330
3 Samuels, R. J. 'Structured Polymer Properties', John Wiley, 1974
4 Allison, S. W. and Ward, I. M. *Br. J. Appl. Phys.* 1967, **18**, 1151
5 Ward, I. M. *Chem. Ind.* 1956, p. 905
6 Heffelfinger, C. J. and Schmidt, P. G. *J. Appl. Polym. Sci.* 1965, **9**, 2661
7 Cunningham, A., Ward, I. M., Willis, H. A. and Zichy, V. *Polymer* 1974, **15**, 749
8 Rietsch, F., Duckett, R. A. and Ward, I. M. *Polymer* 1979, **20**, 1133
9 Cunningham, A. and Davies, G. R. and Ward, I. M. *Polymer* 1974, **15**, 743
10 Huisman, R. and Heuval, H. M. *J. Appl. Polym. Sci.* 1978, **22**, 943
11 Heuval, H. M. and Huisman, R. *J. Appl. Polym. Sci.* 1978, **22**, 2229
12 Nobbs, J. H., Bower, D. I. and Ward, I. M. *Polymer* 1976, **17**, 25
13 Samuels, R. J. *J. Polym. Sci.* 1965, **A-23**, 1741
14 Gupta, V. B. and Kumar, S. *J. Polym. Sci., Polym. Phys. Edn.* 1979, **17**, 1307
15 Biangardi, H. J. *J. Polym. Sci., Polym. Phys. Edn.* 1980, **18**, 903